

again, exchange forces could act to prevent the observed widths and shifts from leveling off.

The observed

$$[\text{shift}(m) + \text{shift}(-m)][\text{width}(m) + \text{width}(-m)]^{3/2}$$

values, instead of being constant as theory predicts, increase then decrease as $|m|$ increases.^{17,24} There is no obvious reason for the increase at low $|m|$. The decrease often occurs when the optical radii—approach or became smaller than the gas-kinetic radii. In He and Ne broadening, however, such a correlation cannot be found, all empirical optical radii being smaller than gas-kinetic from the start.

²⁴ R. M. Herman (to be published).

An experimental determination of the rare-gas-broadened pure rotation [(0-0) band] linewidths and shifts would be worthwhile at the present time. Since first-order phase shifting is not operative in broadening and shifting these lines, the effects of inelastic processes alone could be studied. To extend our calculations to these lines would be routine. However, this step has not yet been taken, inasmuch as comparison with experiment is impossible at the present time.

ACKNOWLEDGMENT

The author wishes to thank Professor Henry Margenau for calling attention to the line-shift problem and for continued helpful guidance throughout the course of this research.

Hyperfine Structure of Hg¹⁹⁷ and Hg¹⁹⁹†

CARL V. STAGER*

Department of Physics and Research Laboratory of Electronics, Massachusetts Institute of Technology, Cambridge, Massachusetts

(Received 7 May 1963)

The hyperfine structure of the 3P_1 state of Hg¹⁹⁷ and Hg¹⁹⁹ has been measured by a microwave-optical experiment. This involves optical excitation to the desired state, paramagnetic resonance in this state, and an optical method of detecting the paramagnetic resonance. The paramagnetic resonances were obtained between different F levels as a function of magnetic field. Quadratic Zeeman corrections were estimated by second-order perturbation theory and the corrected transition frequencies were then extrapolated to zero field. The zero-field hyperfine-structure splittings in the 3P_1 state are Hg¹⁹⁷ ($F = \frac{3}{2}$ to $F = \frac{1}{2}$) = 23 086.37(2) Mc/sec, Hg¹⁹⁹ ($F = \frac{3}{2}$ to $F = \frac{1}{2}$) = 22 128.56(2) Mc/sec. Hyperfine-structure constants A are obtained which are correct to second order. These are combined with the known nuclear magnetic moments to give the hyperfine-structure anomaly in the 3P_1 state: $\Delta(^3P_1, \text{Hg}^{199}, \text{Hg}^{201}) = -0.00147(1)$, and the anomaly of the hyperfine-structure interaction for the 6s electron in the 3P_1 state: $\Delta(s_{1/2}, \text{Hg}^{199}, \text{Hg}^{201}) = -0.00175(9)$.

I. INTRODUCTION

MERCURY has two stable isotopes with nonzero spin, Hg¹⁹⁹ with $I = \frac{1}{2}$ and Hg²⁰¹ with $I = \frac{3}{2}$. Hg¹⁹⁷ is radioactive with a half-life of 65 h. It also has $I = \frac{1}{2}$. The hyperfine structure of the 3P_1 state of Hg²⁰¹ has been measured by Kohler.¹ This work is basically an extension of Kohler's method, applied to Hg¹⁹⁷ and Hg¹⁹⁹. The hyperfine-structure splittings in the 3P_1 state of Hg¹⁹⁷ and Hg¹⁹⁹ have been measured to an accuracy of approximately one part in a million. For both isotopes this represents an increase in the accuracy, over existing measurements, of a factor of approximately 100.

† This work, which is based on a thesis submitted to the Department of Physics, Massachusetts Institute of Technology, in partial fulfillment of the requirements for the degree of Doctor of Philosophy, was supported in part by the U. S. Army, the Air Force Office of Scientific Research, and the Office of Naval Research.

* Present address: McMaster University, Hamilton, Ontario, Canada.

¹ R. H. Kohler, Phys. Rev. **121**, 1104 (1961).

This increase in accuracy permits one to obtain the hyperfine-structure anomaly in the 3P_1 state. The hyperfine-structure anomaly for Hg¹⁹⁹ and Hg²⁰¹ has previously been measured in the 3P_2 state² and by means of the Knight shift.³ The agreement between these results is excellent.

II. APPARATUS AND METHOD

A. Excitation and Detection

The relevant energy levels of the mercury atom are shown in Fig. 1. The 3P_1 state is connected to the 1S_0 ground state by the 2537 Å resonance line. On the right-hand side of Fig. 1, the relative positions of the hyperfine components of the 2537 Å line are shown, including only those isotopes that are relevant for this discussion.

² M. N. McDermott and W. L. Lichten, Phys. Rev. **119**, 134 (1960).

³ J. Eisinger, W. Blumberg, and R. Schulman, Bull. Am. Phys. Soc. **4**, 451 (1959).

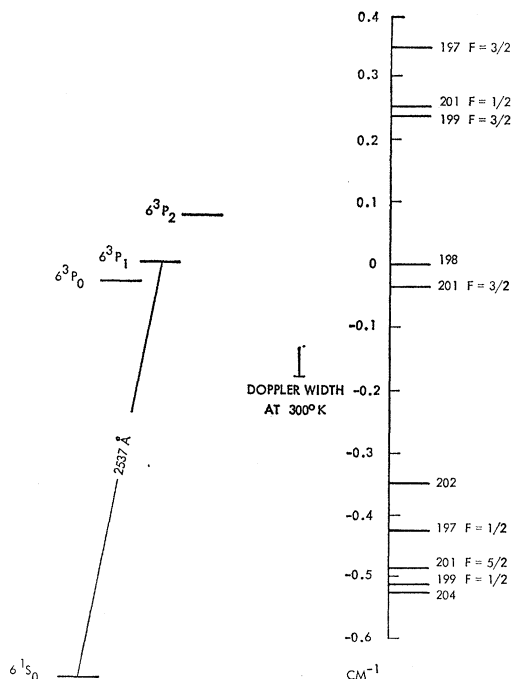


Fig. 1. Left, $6s6p$ triplet energy levels of mercury. Right, relative positions of hyperfine components of 2537 Å line.

On the same scale, the Doppler width of the 2537 Å line at 300°K is shown.

It is easily seen from Fig. 1 that by illuminating Hg^{199} vapor with the 2537 Å line from Hg^{204} only the $F = \frac{1}{2}$ state is excited. Therefore, excitation to the 3P_1 state and the population difference that is necessary for microwave resonances are achieved simultaneously, independently of any polarization or statistical weight effects. When an excited Hg atom reradiates, the frequency depends on whether the atom was in the $F = \frac{1}{2}$ or $\frac{3}{2}$ state. Discriminating between these frequencies

permits one to detect the microwave resonance by optical techniques. Figure 2 gives a simplified diagram of the experimental arrangement, showing exciting lamp, sample cell, filter cell, and photomultiplier. The filter cell contains Hg^{204} vapor and absorbs radiation originating from the $F = \frac{1}{2}$ level. This is the method developed by Kohler and first applied to the measurement of the 3P_1 hyperfine structure in Hg^{201} .¹

Figure 1 shows that there is no fortunate coincidence of energy levels for Hg^{197} like the one exploited in the Hg^{199} experiment. For excitation of Hg^{197} and Hg^{204} discharge was run severely self-reversed. Figure 3 shows the expected lamp intensity output as a function of frequency for the self-reversed condition. The additional peaks are due to other mercury isotopes present in the lamp. The peak intensity of one-half of the self-reversed line coincides approximately with the $F = \frac{1}{2}$ level of Hg^{197} . The filter cell employed a mixture of Hg^{202} and Hg^{204} . Also, argon was added to the filter cell to a pressure of 400 mm. Figure 3 shows the expected absorption coefficient of the Hg^{202} , Hg^{204} mixture, with and without the argon. The curves are plotted from the data given in the review article of Ch'en and Takeo.⁴ The Hg^{204} appears superfluous but was added to prevent any reflected radiation from reaching the photomultiplier and contributing to the shot noise.

B. Optics

The lamp used for excitation was an Hg^{204} electrodeless discharge. The Hg^{204} was approximately 75% enriched and was obtained from Oak Ridge National Laboratories. The principal impurity was 20% of Hg^{202} . The lamp was excited by 10-cm microwaves in a manner similar to that employed by Kohler. The dry nitrogen blast was replaced by continuous-flow water cooling when it was necessary to run the lamp without self-reversal. The filter cell had an absorption length of 2 in.

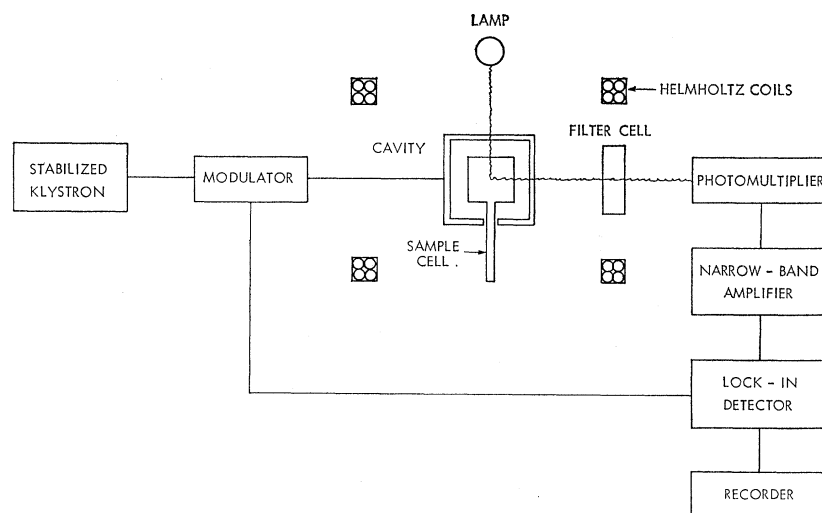


FIG. 2. Experimental arrangement.

⁴ S. Ch'en and M. Takeo, Rev. Mod. Phys. **29**, 20 (1957).

and was made of quartz. The sample cell was made of Electric Quartz supplied by Synchor Products, Malden, Massachusetts. This type of quartz is supposed to contain less water than fused quartz produced by conventional methods. The Electric Quartz was notably less lossy at 23 kMc/sec than conventional fused quartz. The photomultiplier was shielded from visible light by means of a 2537 Å interference filter.

C. Microwave System

For both isotopes a Raytheon 2K33 klystron was employed. It was frequency stabilized to a wavemeter. The frequency of the klystron was measured by beating it against a Gertsch FM-4 microwave frequency multiplier that was, in turn, phase locked to a Gertsch FM-6A frequency meter. The microwave cavity was a right circular cylinder operating in the TE₀₁₁ mode. The end walls were threaded plungers. These plungers were used to tune the cavity to the desired frequency. The microwave power was 100% square-wave modulated by means of a rotating sector passing through a slit in the waveguide.

D. Magnetic Field

A small magnetic field was employed to scan the resonance. This was provided by a pair of 10-in.-diam Helmholtz coils. The field was swept electronically at rates from 0.1–5 G/min to a maximum of 20 G. The magnetic field was not measured accurately in an absolute sense, that is, in gauss. To obtain relative field measurements the coil current was passed through a shunt kept at ice-water temperatures.

E. Samples

The Hg¹⁹⁹ sample was obtained from Oak Ridge National Laboratories as mercuric nitrate in solution. After evaporation the resulting crystals were sealed onto a vacuum system and decomposed by heating under vacuum. The mercury was trapped in the quartz sample cell and then drawn off the system. The method of preparing radioactive Hg¹⁹⁷ and distilling it into a sample cell is a standard technique in our group at the Research Laboratory of Electronics and is described in detail elsewhere.^{5,6}

F. Method of Taking Data

To scan the resonance the microwave frequency was held constant and the magnetic field was scanned. For the Hg¹⁹⁹ experiment the photomultiplier signal, after being amplified and phase-detected, was displayed on one channel of a two-channel recorder. The magnetic field and field-calibration markers were plotted on the other channel. For the Hg¹⁹⁷ experiment the signal was

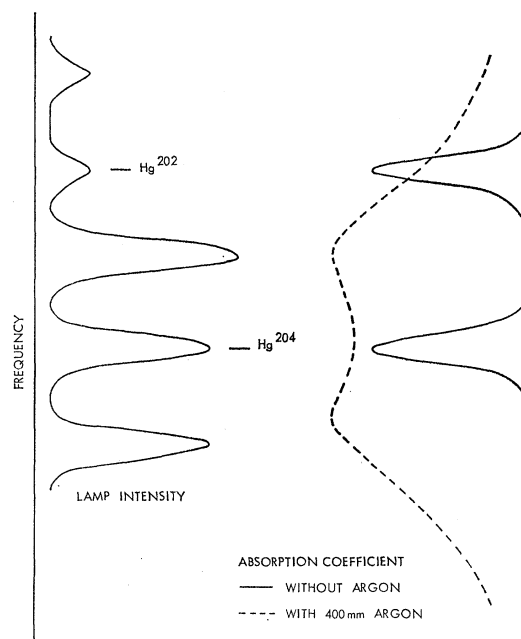


FIG. 3. Left, intensity as a function of frequency for self-reversed lamp containing 75% Hg²⁰⁴ and 20% Hg²⁰². Right, absorption coefficient of filter cell containing Hg²⁰⁴ and Hg²⁰² with and without argon.

applied to the *Y* axis and a signal proportional to the magnetic field to the *X* axis of an *X-Y* recorder.

The TE₀₁₁ cavity was oriented with the rf magnetic field along the axis of the cavity, parallel to the dc magnetic field. Therefore, one would expect only σ transitions ($\Delta F = \pm 1, \Delta M = 0$). Since the sample occupied a

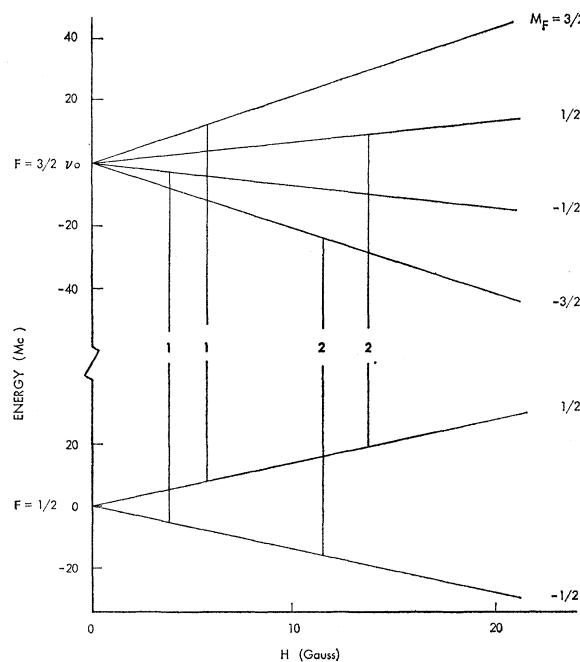


FIG. 4. Zeeman effect of the 3P_1 state.

⁵ A. Melissinos, Ph.D. thesis, MIT, 1960 (unpublished).

⁶ C. Stager, Ph.D. thesis, MIT, 1960 (unpublished).

large fraction of the cavity volume, π transitions could also be observed. All of the data were taken on the σ transition and on the π transition with which the σ transition is degenerate.

Below the zero-field frequency the σ transition ($F=\frac{3}{2}$, $M=\frac{1}{2}$ to $F=\frac{1}{2}$, $M=\frac{1}{2}$) and the transition ($\frac{3}{2}$, $-\frac{3}{2}$ to $\frac{1}{2}$, $-\frac{1}{2}$) were unresolved. They would be degenerate if $g_I=0$. At 10 G the separation between these two transitions is 10 kc/sec, which is much less than the 2-Mc/sec linewidth. The measurements below the zero-field frequency were made on this unresolved pair of transitions. Above the zero-field frequency the ($\frac{3}{2}$, $-\frac{1}{2}$ to $\frac{1}{2}$, $-\frac{1}{2}$), ($\frac{3}{2}$, $\frac{3}{2}$ to $\frac{1}{2}$, $\frac{1}{2}$) pair was used. Figure 4 shows the Zeeman effect of the hyperfine structure for the 3P_1 level for $I=\frac{1}{2}$. The two transitions labeled 2 are those used for frequencies below the zero-field frequency and the two marked 1 were used above the zero-field frequency.

For each frequency four scans of the resonance were taken. One was taken with the magnetic field increasing in magnitude and another with the magnetic field decreasing in magnitude. These two were averaged to eliminate any possible time-constant displacement of the peak. The procedure was repeated with the direction of the magnetic field reversed to cancel out the effect of the earth's magnetic field. These four scans constituted one field-frequency point. Eight field-frequency points were taken for each isotope, four below the zero-field frequency and four above. The approximate field for each point was calculated and the quadratic Zeeman corrections were subtracted from the transition frequencies. The largest quadratic Zeeman correction was 30 kc/sec. The slope of the below zero-field frequency transitions is the negative of the above zero-field frequency transitions. The fields for the field-frequency points below the zero-field frequency were treated as negative. The points were then fitted to a line $\nu=\nu_0+gH$, where H is the voltage across the Helmholtz coil shunt and ν_0 is the zero-field frequency. A least-squares procedure was employed to fit the points.

III. RESULTS AND DISCUSSION

A. Hyperfine-Structure Splitting

Final results for the hyperfine-structure splitting are

$$\begin{aligned}\nu_0(\text{Hg}^{197}) &= 23\,086.37(2) \text{ Mc/sec,} \\ \nu_0(\text{Hg}^{199}) &= 22\,128.56(2) \text{ Mc/sec.}\end{aligned}$$

The errors are the probable errors obtained from the least-squares fit and are really a measure of the consistency of the data. Systematic errors were estimated to be less than the quoted probable error. If one quotes three standard deviations instead of the probable error, one obtains ± 0.1 Mc/sec. In view of the 2-Mc/sec linewidth and the 10:1 signal-to-noise ratio, the error seems reasonable.

The measured hyperfine-structure intervals give uncorrected A values as follows:

$$\begin{aligned}A(^3P_1, \text{Hg}^{197}) &= 15\,390.91(1) \text{ Mc/sec,} \\ A(^3P_1, \text{Hg}^{199}) &= 14\,752.37(1) \text{ Mc/sec.}\end{aligned}$$

The best previous values for these A factors were

$$\begin{aligned}A(^3P_1, \text{Hg}^{197}) &= 15\,387(5) \text{ Mc/sec,}^7 \\ A(^3P_1, \text{Hg}^{199}) &= 14\,745(15) \text{ Mc/sec.}^5\end{aligned}$$

B. Second-Order Corrections

The use of the word uncorrected above signifies that the hyperfine-structure interaction has been taken into account in only the first order. McDermott and Lichten² have evaluated most of the matrix elements that are necessary for the second-order calculation. Values of the constants appearing in the matrix elements were taken from McDermott and Lichten, the exceptions being c_1 and c_2 , which were recalculated as a more accurate g_J value for the 3P_1 state is now available.⁷ The revised values are $c_1=0.437(1)$ and $c_2=0.8996(5)$.

In the calculation of the second-order effects, it is necessary to know $A(^3P_2)$ in order to get a first approximation for a_s , $a_{1/2}$, and $a_{3/2}$. $A(^3P_2)_{197}$ is not known with sufficient accuracy so that it was necessary to assume

$$\frac{a_s(197)}{a_s(199)} = \frac{a_{3/2}(197)}{a_{3/2}(199)} = \frac{A(^3P_1)_{197}}{A(^3P_1)_{199}}.$$

The basic assumption is that there is no hyperfine-structure anomaly. This assumption is only used in the calculation of the off-diagonal matrix elements and should be a good assumption to the accuracy required (approximately one part in a hundred).

After the second-order corrections are subtracted from the measured hyperfine-structure intervals A factors correct to second order are obtained.

$$\begin{aligned}A'(^3P_1)_{197} &= 15\,392.66(15) \text{ Mc/sec,} \\ A'(^3P_1)_{199} &= 14\,754.04(14) \text{ Mc/sec.}\end{aligned}$$

C. Hyperfine-Structure Anomaly

The hyperfine-structure anomaly Δ_{12} is defined as $\Delta_{12}=(A_1g_2/A_2g_1)-1$. Kohler¹ has measured the splittings of 3P_1 state in Hg^{201} . From his data the uncorrected A value is $A(^3P_1)_{201}=-5\,454.569(8)$ Mc/sec. The corrected A value was calculated and the result is $A'(^3P_1)=-5\,454.28(8)$ Mc/sec. The ratio of the nuclear g values is $g_{199}/g_{201}=-2.70902(3)$.⁸ Therefore, $\Delta(^3P_1, \text{Hg}^{199}, \text{Hg}^{201})=-0.00147(1)$. This quantity cannot be compared readily with the work of other experimenters or with nuclear theory. The hyperfine-structure anomaly for the $6s$ electron can be compared with both.

⁷ H. R. Hirsch, J. Opt. Soc. Am. **51**, 1192 (1961).

⁸ B. Cagnac and J. Brossel, Compt. Rend. **249**, 77 (1959).

We define

$$\Delta(s_{1/2}, 199, 201) = [a_s(199)g(201)/a_s(201)g(199)] - 1.$$

It may be easily seen that if we write⁹

$$A(^3P_1) = \alpha a_s + \beta a_{1/2} + \gamma a_{3/2} + \delta a_{3/2,1/2},$$

then

$$\begin{aligned} \Delta_s + \frac{\beta a_{1/2}(201)}{\alpha a_s(201)} \Delta_{1/2} + \frac{\gamma a_{3/2}(201)}{\alpha a_s(201)} \Delta_{3/2} \\ + \frac{\delta a_{3/2,1/2}(201)}{\alpha a_s(201)} \Delta_{3/2,1/2} = \Delta(^3P_1) \left[1 + \frac{\beta a_{1/2}(201)}{\alpha a_s(201)} \right. \\ \left. + \frac{\gamma a_{3/2}(201)}{\alpha a_s(201)} + \frac{\delta a_{3/2,1/2}(201)}{\alpha a_s(201)} \right]. \end{aligned}$$

Since the $p_{3/2}$ wavefunction has a negligible overlap on the nucleus, $\Delta_{3/2}$ and $\Delta_{3/2,1/2}$ are very small. Theoretical calculations of $\Delta_{1/2}$ give a ratio of $\Delta_{1/2}$ to Δ_s of approximately 0.2.¹⁰ The coefficient $\beta a_{1/2}(201)/\alpha a_s(201)$ is also approximately 0.2; thus by neglecting this term only a 4% error is made. Therefore, we may write

$$\begin{aligned} \Delta(s_{1/2}, 199, 201) = \Delta(^3P_1, 199, 201) \\ \times \left[1 + \frac{\beta a_{1/2}(201)}{\alpha a_s(201)} + \frac{\gamma a_{3/2}(201)}{\alpha a_s(201)} + \frac{\delta a_{3/2,1/2}(201)}{\alpha a_s(201)} \right]. \end{aligned}$$

This gives $\Delta(s_{1/2}, 199, 201) = -0.00175(9)$. The quoted error does not include the error caused by neglecting $\Delta_{1/2}$ which is of comparable magnitude. McDermott and Lichten give $\Delta(s_{1/2}, 199, 201) = -0.00164(3)$.^{11,2} The hyperfine-structure anomaly for the 6s electron has

⁹ M. N. McDermott and W. L. Lichten (Ref. 2), combined the $a_{3/2,1/2}$ term with the $a_{3/2}$ term through the factor ξ .

¹⁰ H. H. Stroke, R. J. Blin-Stoyle, and V. Jaccarino, Phys. Rev. **123**, 1326 (1961); Technical Report 392, Research Laboratory of Electronics, MIT, 1961 (unpublished).

¹¹ The value $-0.001728(12)$ given by McDermott and Lichten (Ref. 2) is incorrect. M. N. McDermott (private communication, 1960).

also been obtained from the Knight shift.³ $\Delta(s_{1/2}) = -0.0016(9)$. The above-given results are in excellent agreement.

The formalism of Eisinger and Jaccarino¹² was used to calculate the anomaly for the single-particle model. The result is -0.01 and is much too large. This is hardly surprising, since the single-particle model fails to predict a good value of the moment for Hg²⁰¹. The single-particle predictions for the moments of Hg¹⁹⁹ and Hg²⁰¹ are 0.64 and -1.91 , respectively. The experimental values are 0.50 and -0.56 . Arima and Horie¹³ and Blin-Stoyle and Perks¹⁴ have suggested a nuclear model that is remarkably successful in predicting nuclear moments. The model is based on the single-particle model, small amplitudes of excited state configurations being mixed in with the single-particle ground states. By using this approach, the moment of Hg²⁰¹ has been calculated.¹⁵ Depending on the depth of the potential well used, the values that they obtained range from -0.40 to -0.60 . The experimental value is -0.56 , a considerable improvement over the single-particle value of -1.91 . For Hg¹⁹⁹, where the odd nucleon is in a $p_{1/2}$ orbit, the model employed gives zero admixture coefficients, and the single-particle model value of the moment. Although the configuration mixing approach was not used to calculate the anomaly, the measured value of the anomaly and the nuclear moments were used in a semiphenomenological approach to determine the admixture coefficients.¹⁰ Reasonable admixtures are predicted.

ACKNOWLEDGMENTS

It is a pleasure to acknowledge the guidance and supervision of Professor Francis Bitter. Dr. H. R. Hirsch and Dr. H. H. Stroke contributed a great deal in valuable discussions and laboratory assistance.

¹² J. Eisinger and V. Jaccarino, Rev. Mod. Phys. **30**, 528 (1958).

¹³ A. Arima and H. Horie, Progr. Theoret. Phys. (Japan) **12**, 623 (1954).

¹⁴ R. Blin-Stoyle and M. Perks, Proc. Phys. Soc. (London) **A67**, 855 (1954).

¹⁵ H. Noya, A. Arima, and H. Horie, Suppl. Progr. Theoret. Phys. (Japan) **8**, 33 (1958).